

EFFECTS OF MICROSTRUCTURE ON THE MECHANICAL

PROPERTIES OF Ti-15V-3Cr-3Al-3Sn CASTINGS

W. J. Porter^a, R. R. Boyer^b, and D. Eylon^a

^a University of Dayton, Graduate Materials Engineering,
300 College Park Dr., Dayton, OH 45469-0240, USA

^bBoeing Commercial Airplane Group
P. O. Box 3707, M/S 73-43, Seattle, WA 98124, USA

ABSTRACT

The relationships between microstructure, room temperature tensile strength and fatigue for investment castings of the high strength beta alloy, Ti-15V-3Cr-3Al-3Sn (wt%) (Ti-15-3), were studied. Following hot isostatic pressing (HIP) to close casting-related porosity, various heat treating and aging schemes were used to obtain high strength and high ductility conditions. Static and dynamic mechanical testing yielded tensile strengths ranging from 160 to 170 ksi (1120 to 1190 MPa) and fatigue runout stress levels from 120 to 140 ksi (840 to 980 MPa). In most cases, fatigue crack initiation was found to be associated with the presence of grain boundary alpha phase, with residual casting microporosity playing a lesser role. Thin, continuous, and planar grain boundary alpha phase oriented at about 45° to the applied stress was responsible for the majority of fatigue initiation events. Grain boundary alpha thickness appears to play a role in the formation of tensile voids. Material with thicker grain boundary alpha phase resulted in tensile fracture predominantly along prior beta grains and was associated with lower tensile elongation. The role of grain boundary alpha phase in tensile failure and fatigue crack initiation is discussed, as well as possible methods for controlling its presence.

INTRODUCTION

The lightweight, high strength, and corrosion resistant nature of titanium and titanium alloys has made it a popular candidate material for various engineering applications. However, the inherent cost of titanium requires investigation of more competitive manufacturing methods. Near-net-shape manufacturing processes, such as investment casting and powder metallurgy, were introduced to address the cost issue and are commonly used in the aerospace community. Investment casting is currently the most widely accepted and fastest growing titanium net-shape manufacturing process [1].

Although the majority of current titanium investment castings have involved the α - β alloy Ti-6Al-4V, significant work has also been done in the area of beta titanium castings [1]. Beta alloy castings have received much attention due to their excellent combination of strength, ductility and toughness. With appropriate processing, tensile strengths as high as 180 ksi (1260 MPa) with 9% elongation and runout fatigue strengths as high as 140 ksi (980 MPa) have been obtained for various beta alloys [1-3]. This study examined investment castings of the beta alloy, Ti-15V-3Cr-3Al-3Sn (wt%) (Ti-15-3) obtained from different sources. It evaluated various post-casting hot isostatic pressing (HIP) and heat treatment routes in terms of microstructure and the resulting mechanical properties. Special attention was given to room temperature tensile and fatigue properties.

Parts of this work were funded by Boeing Commercial Airplane Group

Titanium '92
Science and Technology
Edited by F.H. Froes and I. Coplan
The Minerals, Metals & Materials Society, 1993

EXPERIMENTAL PROCEDURES

MATERIAL

The chemical compositions of some of the Ti-15-3 castings used in this study are shown in Table I. The castings came from a number of suppliers and in a wide array of shapes. Some of these cast shapes included oversized blanks with 0.5" (12.5 mm) gage diameter x 3" (75 mm) length, rectangular test bars from 1" x 1" (25 x 25 mm) to 1" x 6" (25 x 150 mm), test plates from 0.15 to 1" (4 to 25 mm) in thickness and step castings increasing in thickness from .125"- .25"- .5"- 1", respectively. More details on this work are available elsewhere [4].

Table I: Compositions of Ti-15V-3Cr-3Al-3Sn Castings Used in This Work

Supplier	Element (wt %)									
	V	Cr	Al	Sn	Fe	O	N	H	C	Ti
A	15.6	3.0	3.0	3.1	0.11	0.125	0.013	0.003	0.009	Bal.
B	14.0	1.8	3.1	2.8	0.10	0.117	0.008	0.013	NA	Bal.
C	14.3	2.6	2.9	2.6	0.10	0.110	0.011	0.002	NA	Bal.
D	14.9	2.9	3.2	2.5	0.12	0.108	0.008	0.006	NA	Bal.

PROCESSING

The various HIP and heat treatment schedules used are shown in Table II. The beta-transus temperature for Ti-15-3 was determined to be $1400 \pm 15^\circ\text{F}$ ($760 \pm 8^\circ\text{C}$) [5]. Condition 1 and 2 specimens were provided by supplier A (Table I). Condition 3 specimens were provided by suppliers B, C, and D.

Table II: HIP and Heat Treatments Used for Ti-15V-3Cr-3Al-3Sn Castings

Condition	HIP Cycle	Solution Treatment	Aging
1	1650°F/15ksi/2hr (900°C/105MPa/2hr)	1750°F/1hr/GFC ^a (955°C/1hr/GFC)	975°F/12hr/AC ^b (525°C/12hr/AC)
2	1750°F/15ksi/2hr (955°C/105MPa/2hr)	1750°F/1hr/GFC ^c (955°C/1hr/GFC)	975°F/8hr/AC (525°C/8hr/AC)
3	1650 or 1750°F/15ksi/2hr (900 or 955°C/105MPa/2hr)	-- none --	975°F/12hr (525°C/12hr)

^aGFC - Gas Fan Cooling 150°F(85°C)/min

^bAC - Air Cool 50°F(30°C)/min

^cGFC - 350°F(195°C)/min

MECHANICAL TESTING

Specimens HIP'd and heat treated according to Conditions 1 and 2 (Table II) were taken from cylindrical casting blanks (Table III). They were machined into a unified tensile and fatigue specimen geometry with a 1.25" (32 mm) gage length, 0.2" (5 mm) gage diameter, and 0.518" (13.2 mm) x 20 threaded grip. Tensile testing was conducted at room temperature with a strain rate of 0.005 min⁻¹ through 0.2% yield, followed by a crosshead speed of 0.05 in (1.3 mm)/min to failure. Multiple bars from each condition were tested (Table III). Condition 3 tensile specimens, which were HIP'd and direct aged, were machined from the oversized cast shapes (Table III).

High cycle fatigue (HCF) (axial load) testing was done at room temperature in laboratory air using a triangular load-time waveform, with frequencies ranging from 20-30 Hz. An R ratio ($R = \sigma_{\min}/\sigma_{\max}$) of 0.1 (tension-tension mode testing) was chosen to preserve fracture surfaces for fractographic analysis. The smooth specimens for the limited fatigue testing of the direct aged material (Condition 3) were taken from 0.5" (13 mm) diameter cast round bars provided by supplier C.

RESULTS

MICROSTRUCTURE

Representative microstructures of Conditions 1, 2, and 3 (Table II) are shown in Figs. 1a, b and c, respectively.

TENSILE PROPERTIES

Room temperature tensile and fatigue properties of Conditions 1, 2 and 3 are listed in Table III. The grain boundary alpha (GB α) thickness of the tensile specimens was measured only for Conditions A1, A2, and C3 (0.5" plate).

Typical tensile fracture surfaces for Conditions 1 and 2 are shown in Fig. 2. These are also representative of Condition 3 fracture surfaces.

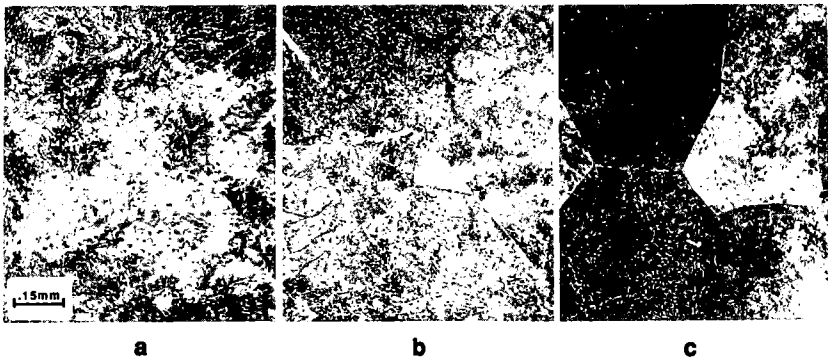


Figure 1: Optical micrographs of Ti-15V-3Cr-3Al-3Sn castings: (a) Condition 1, (b) Condition 2, and (c) Condition 3 as defined in Table II. Original magnification is 100X.

Table III: Mechanical Properties of Condition 1, 2, and 3 Ti-15V-3Cr-3Al-3Sn Castings

Supplier	Cond.	Cast Geometry	UTS ksi (MPa)	.2%YS ksi (MPa)	El. (%)	R.A. (%)	No. of Tests	Fatigue Ratio ^a	Avg. GB α Thickness (nm)
A	1	.5" dia x 3" length bars	181 (1265)	169 (1180)	3.7	9.3	3	0.69	60 \pm 20
	2	.5" dia x 3" length bars	174 (1215)	159 (1110)	6.6	15.0	3	0.70	40 \pm 15
B	3	1" dia. bars	174 (1215)	165 (1155)	4.5	4.5	2	NA	
C	3	over size test bars	181 (1265)	164 (1145)	6.3	9.7	3	0.78	
	3	.375x1x6" test bars	182 (1270)	170 (1190)	7.5	NA	2	NA	
	3	.375x4x6" plate	180 (1260)	167 (1170)	6.3	12.8	4	NA	
	3	0.5" plate	170 (1190)	164 (1145)	2.0	NA	2	NA	200 \pm 25
D		Step casting							
	3	.125" step	181 (1265)	172 (1200)	4.5	5.8	2	NA	
	3	.25" step	176 (1230)	168 (1175)	4.0	4.9	2	NA	
	3	.5" step	174 (1215)	167 (1165)	3.0	3.5	2	NA	
	3	1" step	162 (1130)	158 (1105)	3.0	7.0	2	NA	

^afatigue ratio = runout fatigue strength/ UTS

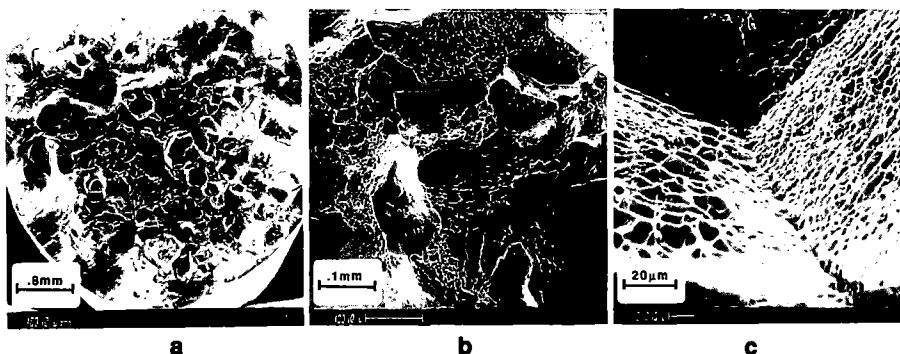


Figure 2: Tensile fracture surfaces of: (a) Condition 1, (b) Condition 2 specimens, and (c) high magnification of Condition 1 highlighting ductile dimpling along GBα fracture surface.

FATIGUE PROPERTIES

A comparison of the high cycle fatigue test data (S-N curves) for smooth fatigue specimens from all three HIP and heat treatment conditions is plotted in Fig. 3.

Condition 1 and 2 fatigue specimens exhibited two types of fatigue crack initiation sites. Examples of the *grain boundary alpha* and *multipore* related initiation sites are shown in Fig. 4.

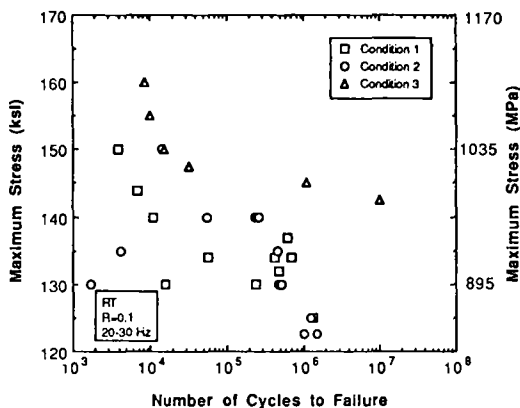


Figure 3: Comparison of high cycle fatigue data for all three HIP+heat treatment conditions.

DISCUSSION

MICROSTRUCTURE

While the room temperature tensile and high cycle fatigue test results indicate that the mechanical properties of Ti-15-3 castings were influenced by changes in the HIP parameters and the subsequent heat treatments, the optical microstructures for the three conditions (Fig. 1) were not significantly different. Each condition resulted in microstructures exhibiting fine alpha precipitates in a recrystallized beta matrix. A small difference in the amount of alpha precipitate between the solution treated Conditions 1 and 2 was noticeable, with Condition 1 having more. This was due to the longer aging time of 12 hours for Condition 1 versus 8 hours for Condition 2.

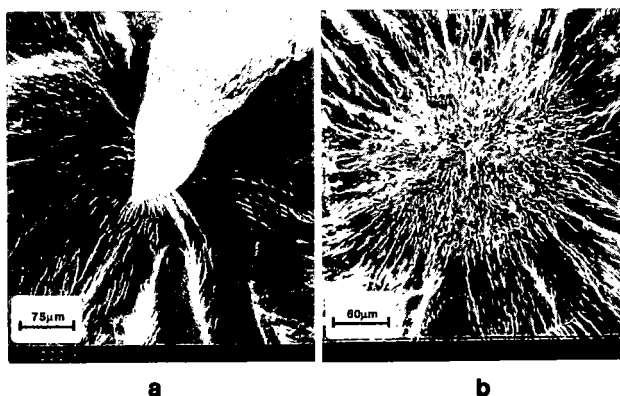


Figure 4: Fatigue crack initiation sites for Conditions 1 and 2: (a) grain boundary alpha at 45° to tensile direction, and (b) micropore on a plane oriented 90° to tensile direction.

One of the most prominent features of the microstructure was the continuous GB α phase on the prior beta grain boundaries. GB α is common in beta solution treated, solute rich, beta titanium alloys such as the Ti-15-3 alloy used in this study [1-3,6,7]. The formation of GB α occurs during cooling through the α - β phase field. Condition 2 exhibited somewhat thinner GB α phase than that found in Condition 1 (40 vs 60 nm, Table III) due to differences in the cooling rates. The faster cooling rate for Condition 2, 350°F(195°C)/min, as opposed to 150°F(85°C)/min for Condition 1, was employed in an attempt to minimize the thickness of the GB α . Ideally, this should lead to improved mechanical properties, such as tensile elongation and fatigue strengths. In Condition 3, the HIP cycle acted as a solution treatment with a very slow cooling rate, leading to formation of the thickest GB α observed in this study (200 nm, Table III). The 975°F(525°C)/12hr direct aging of Condition 3 following HIP, resulted in a microstructure similar to Condition 1, which was also aged for 12 hours at 975°F(525°C) following solution treatment.

TENSILE PROPERTIES

Although the differences in the microstructures of each condition were subtle, their effect on mechanical properties was readily apparent. While both Conditions 1 and 2 were beta solution-treated, the longer aging times for Condition 1 (which led to a larger amount of α -phase precipitation) resulted in higher yield and tensile strengths when compared with Condition 2 (Table III). The short α/β interfaces formed upon precipitation of the alpha in the beta structure acted as effective obstacles to dislocation motion and crack propagation and strengthened the material accordingly [3]. It was also interesting to note the differences in the tensile properties obtained using the direct age (Condition 3). In general, the specimens with the thicker cross sections exhibited lower ductility. This was most notable in the step castings where the section thickness varied from 0.125 to 1" (3 to 25 mm) (Table III). The lower ductility was attributed to the slower cooling rates encountered with thick cross sections and the subsequent formation of large beta grains and thicker GB α [2].

In an attempt to correlate the loss of tensile elongation to the existence of thicker GB α , the thickness of this phase was measured in three microstructural conditions (Table III). These selected conditions represented very low, intermediate, and high tensile elongations [C3 (0.5" plate), A1 and A2, respectively]. The RT tensile elongation was plotted against the GB α thickness in Fig. 5. It should be noted that this study was based on limited data and therefore may only provide a general guideline.

As would be expected, the higher strength of Condition 1 was associated with a corresponding drop in ductility in spite of the very dimpled nature of the fracture surface (Fig. 2c). The drop in ductility was related to the strength differences between the high strength α - β structure material

and the relatively soft GB α regions. The presence of flat and continuous GB α lead to long, relatively soft zones which preferentially deformed and eventually fractured intergranularly during straining (Fig. 2)[2,3]. This resulted in large *localized plastic strains* which were distributed over the relatively small volume of the GB α material [3] (Fig. 2c). Due to the planar nature of the GB α -phase and the corresponding long slip paths found in the β -solution treated and aged (β -STA) material, high stress concentrations and local strains were developed at the grain boundary triple points. The inherent strength of the finely precipitated $\alpha+\beta$ structure enhanced the strain localization in the relatively soft GB α . In these triple point regions, fracture occurred at low *macroscopic strains* even though high *local strains* were accommodated at the GB α as evidenced by the highly dimpled facets (Fig. 2c) [3].

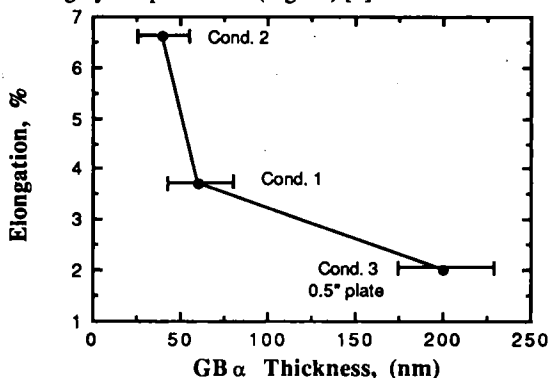


Figure 5: Influence of GB α thickness on room temperature elongation.

A number of factors have been identified to reduce tensile crack nucleation and gain ductility in β -STA beta alloys. These include minimizing the thickness and length of the relatively soft GB α zones and reducing the strength differences between the GB α material and the $\alpha+\beta$ structure. Both issues were addressed by the changes made in the heat treatments from Condition 1 to Condition 2. Condition 2 material was cooled at a faster rate to reduce the thickness of the GB α material. Also, the shorter aging times used in Condition 2 resulted in a lower strength $\alpha+\beta$ structure by reducing the amount of fine alpha phase precipitation. Therefore, lower strength differences between the GB α and the $\alpha+\beta$ structure resulted in higher tensile elongation.

The relatively small reduction in tensile strength from Condition 1 to 2 was associated with a twofold increase in elongation (Table III). It was also associated with a change in fracture mode from dimpled *intergranular* fracture (Condition 1, Fig. 2a) to predominantly dimpled *transgranular* fracture (Condition 2, Fig. 2b). The high strength of Condition 1 localized the deformation in the relatively soft GB α leading to a highly ductile but localized fracture zone along the prior beta grains at the GB α phase. On the other hand, the lower strength Condition 2 resulted in more plasticity in the $\alpha+\beta$ matrix structure, leading to more macrodeformation throughout the sample and hence the higher tensile elongation.

It is also possible to correlate the room temperature elongation to the GB α thickness since a thick GB α will increase the strain localization into the lower strength zone. As can be seen from Table III, the lowest elongation (Condition 3- 0.5\" plate) was associated with a 200 nm average GB α thickness, while the highest elongation (Condition 2) displayed only a 40 nm average thickness as illustrated in Fig. 5. Similar findings have been reported for $\alpha+\beta$ alloys where tensile voids in the GB α zone were shown to grow at faster rates as GB α thickness increased [8].

FATIGUE PROPERTIES

Condition 2 displayed slightly better fatigue ratio (Table III) than Condition 1. In both conditions the fatigue cracks initiated internally in most of the specimens tested (Fig. 4). This was unusual since fatigue crack initiation is typically a surface-related phenomena.

The most common initiation site in both conditions was along the GB α phase. A feature common to the GB α -initiated cracks was long, planar and continuous GB α inclined about 45° to

the tensile direction (Fig. 4a), coinciding with the angle of maximum shear stress. Initiation sites with similar characteristics have been reported for Ti-6Al-4V [9] and for the beta alloy, Ti-8Mo-8V-2Fe-3Al [10].

Thick, planar regions of GB α oriented near 45° to the direction of applied stress nearly always accounted for loss of fatigue life in Ti-6Al-4V [9], which agrees with the results of this work. While Condition 2 samples had lower UTS than Condition 1 samples [174 (1215) vs 181 ksi (1265MPa)], the fatigue ratio ($S=\sigma_f/\sigma_{UTS}$) was higher for Condition 2 than Condition 1. The higher fatigue ratio indicated a lower propensity to nucleate cracks at GB α due to the relatively lower α - β matrix strength. This may also be the result of the thinner GB α in Condition 2 versus the thicker GB α in Condition 1.

About 15% of initiation sites were associated with residual casting micropores. The fact that micropores were not readily evident in any of the tensile specimens examined is an indication that there were probably only very few present due to HIP. Further, most of these pores were 10 to 15 μ m in diameter (Fig. 4b). The microporosity responsible for fatigue crack initiation was always found on GB α fracture facets. This fact links pore initiation to GB α initiation. Micropore-initiated fatigue cracks do not necessarily start at GB α oriented 45° to the stress direction since the pore stress risers were sufficient to initiate cracks at other orientations. It was very intriguing that *all* samples associated with *micropore initiation* exhibited *above average* fatigue lives. It is possible that the samples exhibiting micropore-initiated failure had correspondingly thin or non-planar regions of GB α , so that initiation shifted to the next weakest link: the areas of stress concentration surrounding the micropores.

The fatigue ratios for all conditions, Condition 1- $S = 0.69$, Condition 2- $S = 0.70$, and Condition 3 - $S = 0.78$ (Table III) are similar to those found in another beta alloy, Beta C, and are generally superior to cast+HIP Ti-6Al-4V. Ti-6Al-4V typically range from 0.65 to 0.71 [1].

The high strength and fatigue properties, in addition to the low densities, of the beta titanium alloys make them an attractive option to replace precipitation-hardened steel castings such as 17-7 PH. However, additional work is needed to reduce property scatter, particularly low fatigue lives and low tensile elongation. Controlling the formation of GB α phase will be required to meet these challenges and increase the aerospace applications of the β alloys.

SUMMARY AND CONCLUSIONS

Investment castings of the high strength beta titanium alloy, Ti-15V-3Cr-3Al-3Sn (Ti-15-3), were studied to determine the tensile and fatigue behavior and the mechanisms leading to tensile and fatigue crack initiation. Three conditions were examined by applying different hot isostatic pressing (HIP), solution treating and aging parameters.

1. The three process conditions provided relatively high ultimate strengths in the range of 160 (1120) to 180 ksi (1260 MPa).
2. The lower strength Condition 2 material showed an almost twofold increase in tensile elongation over Condition 1 material. The tensile fracture surface of the Condition 1 showed a highly faceted, ductile, intergranular mode of failure while the Condition 2 fracture surface was somewhat faceted and exhibited a higher percentage of transgranular fracture.
3. The large strength mismatch between the finely precipitated α - β structure and the grain boundary alpha (GB α) phase in Condition 1 resulted in localized ductile intergranular tensile fracture surfaces yet with low *macrodeformation*. The smaller strength mismatch in Condition 2 allowed for more transgranular deformation and therefore higher elongation.
4. Limited data correlated the tensile elongation to the GB α thickness. Condition 3 with the thickest GB α phase displayed the lowest elongation while Condition 2 with the thinnest GB α phase had the highest tensile elongation.
5. Fatigue cracks initiated at GB α phase for Conditions 1 and 2 and was sometimes associated with occasional residual casting microporosity.

6. GB α fatigue crack initiation was due to the presence of a thin, continuous, planar GB α phase oriented at about 45° to the direction of the applied stresses. GB α initiation resulted in premature fatigue failure for each condition.

7. Fatigue cracks that initiated at micropores were observed only in specimens exhibiting longer than average fatigue lives. These were always associated with GB α regions normal to the tensile direction.

8. The combination of high tensile strength, fatigue strength, and low density will make castings of the beta titanium alloy, Ti-15-3, strong candidates for replacing castings of precipitation-hardened steels (PH) in demanding aerospace and industrial applications.

REFERENCES

1. D. Eylon, W. J. Barice, R. R. Boyer, L. S. Steele, and F. H. Froes, "Casting of High Strength Beta Titanium Alloys," Sixth World Conference on Titanium, Part II, P. Lacombe, R. Tricot, and G. Beranger, eds., Les Editions Physique, Les Ulis Cedex, France, 1989, pp. 655-660.
2. R.R. Boyer, W.J. Porter, and D. Eylon, "Microstructure/Properties Relationships in Ti-15V-3Cr-3Al-3Sn High Strength Castings," Microstructure/Property Relationships in Titanium Aluminides and Alloys, Y-W. Kim and R. R. Boyer, eds., TMS, Warrendale, PA, pp. 511-520.
3. G. T. Terlinde, T. W. Duerig, and J. C. Williams, "Microstructure, Tensile Deformation and Fracture in Aged Ti-10V-2Fe-3Al," Metallurgical Transactions A, Vol. 14A, October 1983, pp. 2101-2115.
4. W. J. Porter, Crack Initiation in Beta Titanium Castings, Master's Thesis, Graduate Materials Engineering, University of Dayton, June, 1990.
5. P. J. Bania, G. A. Lenning, and J. A. Hall, "Development and Properties of Ti-15V-3Cr-3Sn-3Al (Ti-15-3)," Beta Titanium Alloys in the 1980's, R. R. Boyer and H. W. Rosenberg, eds., TMS-AIME, Warrendale, PA, 1983, pp. 209-229.
6. T.W. Duerig and J. C. Williams, "Overview: Microstructure and Properties of Beta Titanium Alloys," Beta Titanium Alloys in the 1980's, R. R. Boyer and H. W. Rosenberg, eds., TMS-AIME, Warrendale, PA, 1983, pp. 19-67.
7. S. Ankem and S. R. Seagle, "Heat Treatment of Metastable Beta Titanium Alloys," Beta Titanium Alloys in the 1980's, R. R. Boyer and H. W. Rosenberg, eds., TMS-AIME, Warrendale, PA, 1983, pp. 107-126.
8. M. A. Greenfield and H. Margolin, "The Mechanism of Void Formation, Void Growth, and Tensile Fracture in an Alloy Consisting of Two Ductile Phases," Metallurgical Transactions, Vol. 3, October 1972, 2649-2659.
9. D. Eylon, "Fatigue Crack Initiation in Hot Isostatically Pressed Ti-6Al-4V Castings," Journal of Materials Science, Vol. 14, 1979, pp. 1914-1922.
10. R. Chait and T. S. Desisto, "The Influence of Grain Size on the High Cycle Fatigue Crack Initiation of a Metastable Beta Ti Alloy," Metallurgical Transactions A, Vol. 8A, June 1977, pp. 1017-1020.